Stabilization of defects by the presence of hydrogen in tungsten: simultaneous W-ion damaging and D-atom exposure

E.A. Hodille, S. Markelj, T. Schwarz-Selinger, A. Založnik, M. Pečovnik, M. Kelemen, C. Grisolia

HAL Id: hal-02263759

https://amu.hal.science/hal-02263759v2

Submitted on 6 Nov 2019

Stabilization of defects by the presence of hydrogen in tungsten: simultaneous W-ion damaging and D-atom exposure

E. A. Hodille[a], S. Markelj[*b], T. Schwarz-Selinger[c], A. Založnik[b], M. Pečovnik[b], M. Kelemen[b,d], C Grisolia[e]

[a]*Department of Physics, University of Helsinki, P. O. Box 43, FI-00014, Finland*
[b]*Jožef Stefan Institute, Jamova cesta 39, 1000 Ljubljana, Slovenia*
[c]*Max-Planck-Institut für Plasmaphysik, Boltzmannstrasse 2, D-85748 Garching, Germany*
[d]*Jozef Stefan International Postgraduate School, Jamova cesta 39, 1000 Ljubljana, Slovenia*
[e]*CEA, IRFM, F-13108 Saint Paul Lez Durance, France*

Abstract

The possible mutual influence and synergistic effect between defect production and the presence of hydrogen isotopes in the crystal lattice of tungsten is studied. For this purpose, we perform modelling of experimental data where polycrystalline tungsten samples were in one case sequentially irradiated by 10.8 MeV tungsten ions followed by low energy deuterium exposure and in the other case simultaneously irradiated by tungsten ions while exposed to deuterium atoms. Modeling of the measured deuterium depth profiles and thermal-desorption spectra for different irradiation temperatures is performed by the MHIMS (migration of hydrogen isotopes in materials) code. A model of trap creation due to tungsten ion irradiation during the deuterium atom exposures is implemented. In both experimental series, the deuterium desorption peaks corresponding to defects induced by tungsten irradiation are described by the same two de-trapping energies of 1.83 eV and 2.10 eV. The experiments give and unambiguous proof that the presence of deuterium increases the overall trap density. The modelling reveals that the two trap concentrations are affected differently by the temperature and the presence of deuterium: The concentration of the low energy trap is significantly higher in the case of simultaneous exposure as compared to sequential exposure especially at high temperature (2.2 times higher at 1000 K). The concentration of the high energy trap is only weakly affected by the presence of hydrogen.

*Corresponding author: sabina.markelj@ijs.si

1. Introduction

Hydrogen interaction with materials plays a crucial role in fusion research as the tritium inventory needs to be controlled inside a future reactor and maintained below specific limits for safe and fuel-efficient operation. Current fusion development concepts aim to produce energy in a closed tritium fuel cycle [1]. The plasma facing components of a fusion reactor like DEMO need to operate at elevated temperatures (< 1500 K) and withstand intense heat loads up to 20 MW/m^2 and large particle fluxes up to 10^{24} part/m^{2}s [2, 3]. Within the expected operational duty cycles the displacement damage from irradiation by energetic 14.1 MeV neutrons produced by the deuterium-tritium fusion reaction (D + T → He (3.5 MeV) + neutron (14.1 MeV)) is anticipated to be few displacements per atom per year [4], adding additional challenges to material choices. Based on these considerations, tungsten (W) and tungsten-based alloys have been proposed as materials to be used as plasma facing components. The hydrogen isotope (HI) inventory in tungsten needs to be predicted for the harsh conditions that will take place in a future fusion reactor, necessarily taking into account also the effect of neutrons. One consequence of neutron irradiation will be the creation of lattice defects by displacing lattice atoms. This displacement damage acts as trapping sites for HIs because of high de-trapping energies compared to the energy barrier attributed to diffusion of solute HIs between interstitial sites. These traps have a strong impact on the overall tritium retention as predicted by rate equation simulations of tritium retention in W during realistic tokamak cycles [5]. During fusion reactor plasma operation both implantation of energetic hydrogen isotope ions and neutrals as well as damage creation by neutron irradiation will take place at the same time. The influence of the presence of HIs during damage creation on defect structure and on fuel retention is still not well understood. Dedicated experiments as well as theory are needed to address these extreme conditions [6, 7]. However, there is currently no facility capable of replicating the extreme operating environments of high particle and heat fluxes, large time-varying stresses, and large fluence of 14.1 MeV fusion neutrons [6].

To study the influence of material displacement damage on fuel retention, high energy ions are used [8] as a surrogate for the displacement damage that neutron irradiation will cause. It has been shown that fuel retention both in fission neutron-damaged [9] and in W-ion-damaged tungsten (so-called self-damaged W) is strongly increased as compared to undamaged tungsten (e.g. [10, 11]).

In this paper we model the deuterium depth profiles presented in [12] together with thermal-desorption spectra derived from these samples after exposure using the MHIMS code [13]. Namely, simultaneous W-ion irradiation and D-atom exposure were performed at different elevated temperatures and the results are compared to the sequential procedure of W-ion irradiation at elevated temperatures followed by D-atom exposure. From the deuterium depth profile absolute trap densities and trap profiles were deduced. From the thermal desorption spectroscopy (TDS) de-trapping energies and trap densities of the individual traps are derived. Modeling the TDS spectra and D depth profiles of the simultaneous and the sequential procedures gives us the possibility to study the influence of the presence of deuterium during damage creation on the evolution of individual traps with sample temperature.

2. Experiment

The details of sample exposures and deuterium depth profiling were already given in [12]. Here only a short overview of the experimental procedure and conditions will be given together with the necessary information not yet provided in [12]. Polycrystalline hot-rolled tungsten samples (PW) manufactured by Plansee with a purity of 99.997 wt. % were used in the present experiment. Samples were recrystallized before the experiment to enlarge grain size to about 50 µm and to reduce the density of natural defects present in the samples.

In order to study the effect of the presence of HI in the material on damaging two experimental procedures were performed in the INSIBA chamber at the 2 MV Tandem accelerator at Jožef Stefan Institute (JSI), Slovenia: *sequential W-ion irradiation at elevated temperatures and D-atom exposure afterwards* (in short: sequential W/D exposure) and *simultaneous W-ion irradiation and D-atom exposure* (in short: simultaneous W/D exposure). In both experimental procedures – sequential W/D as well as simultaneous W/D - the samples were irradiated with the same tungsten energy, flux, and fluence. Irradiation by 10.8 MeV W^{6+} tungsten ions for four hours to a fluence of 1.4×10^{18} W/m^2 creates a damage dose of 0.47 dpa_{KP} at the peak maximum (calculated by SRIM program with the Kinchin-Pease calculation option, 90 eV displacement energy, evaluating the "vacancy.txt" output). This yields a displacement rate of 3.3×10^{-5} dpa/s.

Also the energy (0.28 eV) and flux of the beam of neutral D atoms (5.4×10^{18} D/m^2s) was identical in all cases. D atoms were created by thermal dissociation of molecules in a hot (2100 K) tungsten capillary of a hydrogen atom beam source (HABS) [14]. Exposure of tungsten to low-energy D atoms is one of the most gentle ways of decorating existing defects with hydrogen isotopes without producing any additional damage as in the case of plasma loading or annealing significant amounts of defects that takes place during high temperature gas loading. Hence, the exposure to D atoms is used here as a tool to populate the traps created beforehand in the sample and from D retention and desorption it is then possible to deduce the trap concentrations and de-trapping energies.

Deuterium depth profiles were measured by nuclear reaction analysis (NRA) utilizing a ^{3}He beam. The analyzing beam was 2 mm in diameter which was smaller compared to the size of the W ion beam being 4 mm in diameter. The D depth profile analysis was performed at the central position of the W irradiation beam and D fluxes are also quoted for this position.

For the sequential W/D exposure the sample temperatures were 300 K, 600 K, 800 K and 1000 K. After damaging, all the samples were exposed at 600 K sample temperature for 24 h to D atoms corresponding to a fluence of 4.7×10^{23} D/m^2.

The simultaneous experiment was performed at five different temperatures of 450 K, 600 K, 800 K, 900K and 1000 K. The D-atom exposure started in these cases 20 min before the beginning of the W-ion irradiation. After the end of the W-ion irradiation the sample heating was stopped first. D exposure was ended only when the sample temperature was well below the exposure temperature to avoid thermal losses of D. Since rate equation modelling revealed that this temperature evolution influences the final D atom depth distribution in the material significantly for experiments at 800 K, 900 K and 1000 K, we specify here for all individual exposures at which temperature the D atom flux was terminated. Namely, the D-atom exposures were stopped after approximately 3 min at 420 K sample temperature in the 450 K case, at 490 K for the 600 K case, at 610 K for the 800 K, at 690 K for the 900 K and at 750 K for the 1000 K case. After four hours of damaging NRA was conducted to measure the D depth profile. After this analysis, the samples were exposed to D atoms again at 600 K sample temperature for 19 hours, yielding a fluence of 3.7×10^{23} D/m^2. The purpose of this additional exposure was again to use the D retention (defect population by D atoms) as a measure for the quantity of defects actually created in the material during the simultaneous W/D exposure. Namely, the depth profiles obtained after the first 4 hours gave us only the information on how deep D penetrated during the simultaneous W/D exposure. The absolute D retention is in this case no measure for the trap concentration, since the D atom fraction changes strongly with the exposure temperature. The higher the temperature during D exposure, the more efficient thermal de-trapping of D is and hence the lower the retention. In addition, choosing 600 K for the sample temperature for this additional exposure to D atoms, allowed us to quantitatively compare the depth profiles and the D concentrations in the material for both experimental procedures. In [12] it was observed that deuterium retention remained constant above 900 K for the simultaneous W/D exposure. To make sure this observation is reproducible additional experiments at higher temperature were conducted. One sample was exposed to simultaneous W/D at 1000 K and one at 1130 K sample temperature. In these two cases the W ion flux was two times higher and hence the exposure time was adjusted to half the time to reach the same final damage dose of 0.47 dpa$_{KP}$. With the additional experiments performed, this effect of stabilization was confirmed, not showing a decrease of the maximum D atom concentration above 900 K. Namely, the maximum D concentrations obtained were 0.17 ± 0.01 at. % at 1000 K and 0.16 ± 0.01 at. % at 1130 K what is similar to D concentration measured in the first simultaneous measurements where 0.155 at.% was obtained for 900 K and 1000 K [12].

After the NRA analysis at JSI the samples were analyzed at Max-Planck-Institut für Plasmaphysik (IPP), Garching, Germany with NRA using a ^{3}He beam with 1 mm beam size to measure the lateral homogeneity of deuterium along both axes of the sample. As deuterium retention is small outside the self-damaged area the size of the W beam diameter could also be deduced by that.

Finally thermal-desorption spectroscopy (TDS) was performed on the samples in the quartz tube of the TESS set-up at IPP. A basic description of TESS is given in [15]. A linear oven ramp of 15

K/min up to a maximum temperature of 1323 K was used. Samples were held at the highest temperature for 30 min. The desorbed gases were measured with a Pfeiffer/Inficon DMM 422 quadrupole mass spectrometer (QMS). The secondary electron multiplier of the QMS was operated in single ion counting mode to avoid background noise and to be able to apply Poisson statistics for determining the accuracy. The following 15 mass channels were recorded as a function of time (so-called multiple ion detection mode of the QMS): m/z = 1, 2, 3, 4, 12, 14, 16, 17, 18, 19, 20, 28, 32, 40, and 44. Release was dominated by mass channel 4 and 3. Mass channels above 4 showed no significant release of deuterium containing species. Residual background contributions were determined in a preceding and a consecutive temperature ramp without a sample or an outgassed sample in the heating zone of the glass tube, respectively. Measurements showed only negligible contributions in mass channel 4 at elevated temperatures stemming from helium penetrating through the quartz and contributions on the percentage range for mass channel 3 from residual HD in the system. Both backgrounds were not subtracted from the real desorption signal as they were not visible on a linear scale. Absolute calibration of D_2 desorption was performed by a D_2 calibration gas bottle with a calibrated leak rate of $1.2234 \times 10^{14} D_2$ molecules/sec [16] after each TDS run to account for any possible drifts in the sensitivity of the system. The calibration factor for HD was experimentally determined by flowing either D_2 or HD gas through an orifice of know size from a calibrated volume into the QMS vessel. Based on the pressure recording of a spinning rotor gauge the calibration factor in measured QMS counts per molecule for HD was 110 % of the one derived for D_2. Contribution of HD on the total D desorption was between 25 and 30 %. A reproducibility of the total signal heights of 3 % was derived by consecutive calibration measurements and is governed by the stability of the detector. The accuracy for the absolute amount of D is hence determined by the stated accuracy of the leak valve of 4.6% for the measurement shown here. The temperature response of the samples to the linear oven temperature ramp was calibrated in an independent experiment by a thermocouple spot-welded to one of the tungsten samples after the TDS experiments and this calibration curve was applied to all preceding measurements.

The obtained D desorption spectra are shown in fig. 3 for the simultaneous W/D samples after additional D exposure and in fig. 5 for the sequential W/D experiments. They represent the sum of

deuterium desorption from HD and D$_2$. All TDS spectra show a dominating peak with a high temperature shoulder of different height. Desorption starts only above the exposure temperature of 600 K with maximum desorption taking place around 800 K. More details will be discussed together with the simulation results in section 3.

3. Simulations

To simulate both experimental procedures, we employed the MHIMS code [13], using the surface model [17] developed to handle low energy hydrogen atom exposures. This code is based on a 1D macroscopic rate equation (MRE) model widely used to tackle implantation and desorption of hydrogen isotopes in W like in the TMAP7 code [18] or the TESSIM code [19, 20]. The model implemented in MHIMS as well as its parameters are reported in table 1 of [17]. We used here the classical version of the model in which each trap is characterized by a single de-trapping energy and can only be occupied by one hydrogen atom. It is different from DFT results showing that a defect (for instance a vacancy) can trap several hydrogen atoms with different de-trapping energies depending on the number of trapped atoms [21, 22, 23, 24]. However, Schmid et al. [25] found out that, if one considers only one hydrogen isotope, the results from a fill-level-dependent model are not discernable from the one given by a classical model. As no isotopic exchange experiment is simulated here, the classical model is used. First the free parameters of this model are adjusted. They are then discussed and compared to literature data of DFT and previous MRE simulation results.

The MHIMS free parameters are the relevant energies for D at the surface (desorption energy E_D, migration barrier E_A from the surface to the bulk and E_R from the bulk to the surface energy), and the de-trapping energies $E_{t,i}$ from the traps created by W damaging and their concentrations n_i (m^{-3}). In the following text they are called in the 'self-damaged traps'. In the case of sequential W/D exposure, these traps exist before D exposure and they are considered as static. In the case of simultaneous W/D exposure, these traps are initially absent in the material and are only created during W irradiation. To simulate this dynamical creation of traps, a creation model has been implemented in MHIMS for the self-damaged traps. This model has a similar formalism as the one proposed by Ogorodnikova et al. [26] to simulate ion-induced traps: if one calls $n_i(x, t)$ the concentration of a self-damaged trap type i (in m^{-3}), at time t and depth x, characterized by a trapping energy $E_{t,i}$, its evolution with time is given by equation (1).

$$\frac{dn_i(x,t)}{dt} = \varphi_W \left(f(x) - \frac{n_i(x,t)}{n_{i,max}} \right) \eta_i \qquad (1)$$

where

- φ_W (m^{-2}s^{-1}) is the implantation flux of W ions,
- $f(x)$ (dimensionless) is the depth (x) distribution of the created traps.
- $n_{i,max}$ (m^{-3}) is the maximum concentration of self-damaged trap of type i can reach,
- η_i (m^{-1}) is the creation probability of traps. It is assumed to be same for all traps $\eta_i = \eta$

The steady state of this equation gives a depth distribution of the self-damaged traps as $n_i(x, t \rightarrow \infty) = n_{i,max}f(x)$. No damage is induced deeper than about 1.5 µm which is the calculated range of the damaging zone for 10.8 MeV W ions [12]. We choose for $f(x)$ a functional behavior as shown in figure 1. This model does not reproduce the peaked distribution of dpa given by SRIM but reproduces the typical final depth distribution of D concentration in the damaged layer [10, 27]. In addition, at higher W fluence deuterium retention reaches saturation and the profile is hence expected to flatten. The maximum value of $f(x)$ is 1 meaning that n_i converges to $n_{i,max}$ being the maximum of the concentration of self-damage trap i.
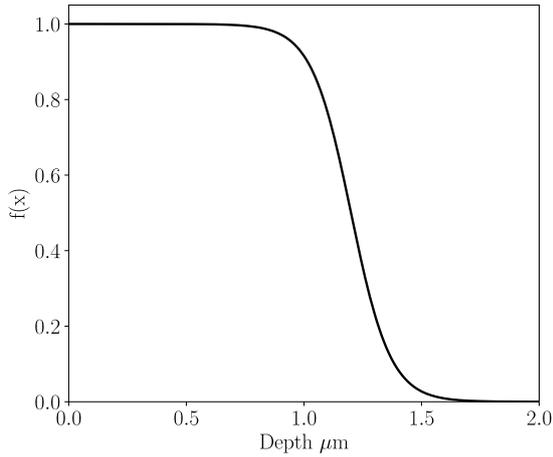

Figure 1. Depth distribution f(x) of created self-damaged traps.

A saturation limit of created defects is used since it was observed experimentally in several publications that there is a saturation of D retention for damage levels above 0.1 dpa [11, 28, 29]. 'tHoen et al. [28] observed saturation for a W fluence above 3×10^{17} Wm^{-2} for 12.3 MeV self-damaging at room temperature. In the experiments simulated in this paper, the W fluence is much higher (1.4×10^{18} Wm^{-2}). Thus, it is most likely that the concentrations of self-damaged traps are saturated in the damaged zone in the course of the experiment. In the current creation model, this saturation is expressed by $n_{i,max}$. In the simple current model, for a constant flux φ_W, the concentration of created traps evolves with the W fluence Φ_W as follows: $n_i(\Phi_W, x) = f(x)n_{i,max}(1 - \exp\left(-\frac{\Phi_W}{\Phi_W^i}\right))$ with $\Phi_W^i = \frac{n_{i,max}}{\eta_i}$ (Wm^{-2}) being the characteristic W fluence governing the growth of n_i. The conversion probability η is chosen such that for a W fluence of 3×10^{17} Wm^{-2} the total trap density reaches 95 % of

the maximum density, meaning that it can be considered as saturated. One obtains $\eta \approx \frac{5\times10^2}{\int f(x)dx}$ (in m^{-1}) for all self-damaged traps, meaning that each W ion creates 5×10^2 traps in the damaged zone. Two papers [28, 29] report this saturation effect for damaging at room temperature. It is assumed that such saturation also occurs at higher temperature. However, the saturation fluence might be different for simultaneous W/D exposure and might depend on the concentration of hydrogen inserted in the materials. Answering these different statements would require additional experiment which is not the scope of the current work.

The surface model is similar to the one presented in [17, 20]. In order to reproduce accurately the experimental data during the simultaneous exposure, a dependence of E_D (desorption) and E_A (from surface to bulk) on the surface concentration of deuterium has been added to the surface model motivated by both experimental [30, 31, 32] and theoretical (DFT) results [33, 34]. With the help of the surface model and the experimental data the migration barrier for D to move from the surface to the bulk is determined as a function of exposure temperature. It is shown that there is a temperature dependence of the migration barrier which at high temperatures and low hydrogen atom surface coverages stabilizes at 2 eV being in good agreement with first-principle DFT calculations [22, 35, 36, 37] and the Fraunfelder experiment [38]. The detail description of this new feature to the model can be found in [39].

Each simulated simultaneous W/D experiment can be divided into three main steps:

- A simultaneous D/W exposure (at 450 K, 600K, 800 K, 900 K or 1000 K) for 4 hours and cooling down to room temperature. The atom flux is $\Gamma_{atom} = 5.4 \times 10^{18}$ m^{-2}s^{-1}. The flux of W ions is $\varphi_W = 9.7 \times 10^{13}$ Wm^{-2}s^{-1}.
- An additional D-atom exposure at 600 K for 19 hours and a cool down to room temperature after the given hold time. The atom flux is the same as in the first phase of the experiment.
- A TDS with a heating ramp of 15 K/min to 1323 K.

Between two different steps, a "storage" phase (e.g. no exposure flux and constant temperature) is simulated that lasts several thousands of seconds so the system evolves to a realistic kinetic equilibrium where the mobile and weakly bonded particles are removed from the system before any TDS or re-exposure. These storage phases are done at 300 K. The temperature is cooled down to 300 K with the same evolution as measured in the experiments. It is particularly important to simulate the correct decrease of sample temperature after the simultaneous D/W exposure, especially for exposure at 800 K, 900 K and 1000 K, as the flux of D atoms is switched off about 3 minutes after the decrease of the temperature. As it will be explained in the following, for the highest exposure temperatures, this delay could induce an increase of the deuterium concentration in the first hundred nanometers observed in the experiments just after the simultaneous exposures (figure 3).

Simulations of sequential W/D exposure include the following steps:

- W exposure (at 300 K, 600K, 800 K, 1000 K) for 4 hours and cooling down to room temperature. The flux of W ions is $\varphi_W = 9.7 \times 10^{13}$ Wm^{-2}s^{-1} (this step is simulated by starting the D exposure with a fixed concentration of traps in the damaged layer).
- A D-atom exposure at 600 K for 24 hours and a cool-down to room temperature. The atom flux is $\Gamma_{atom} = 5.4 \times 10^{18}$ m^{-2}s^{-1}.
- A TDS with a heating ramp of 15 K/min to 1323 K

In both damaging experiments 10.8 MeV W ions are used with the same dose. Thus, the distribution of self-damaged traps in both sets of simulations are the same (figure 1). Consequently, if one observes a difference in terms of trap nature or trap concentration, this would only be due to the influence of deuterium during the trap creation processes.

4. Simulation results

4.1 Simulation of simultaneous W/D exposure experiments

a. Determination of trap concentrations and energies

This section is devoted to the determination of the free trapping parameters for the simultaneous exposure experiments i.e. the de-trapping energies $E_{t,i}$ and the trap concentrations n_i. Similarly to what has been done in [17], the undamaged part of the material is simulated by two intrinsic traps with de-trapping energies of 0.85 eV and 1.00 eV with a trap concentrations of 0.01 at.% each. As already discussed in [17], due to their low de-trapping energy, these two traps do not affect the TDS spectra obtained after a D atom exposure at 600 K.

Based on the shape of the TDS spectra which show only one main peak with a high temperature shoulder, the damaged layer is simulated with only two additional traps. Their de-trapping energies and trap concentrations are determined by reproducing experimental TDS spectra and NRA depth profiles. The values used in the simulations are reported in table 1. The energies reported there are the average of all the de-trapping energies derived in the individual simulations for different temperatures. The scattering of the de-trapping energies around these averages are given by the accuracy reported in this table. Figure 2 shows the comparison between the experimental and simulated deuterium depth profiles (a) and TDS spectra (b). Due to the ambiguity of the size of the W irradiation beam (being elongated and not circular) we did not attempt to convert absolute deuterium desorption flux during TDS to a deuterium desorption per surface area. For this reason, we will only determine the de-trapping energy and the relative concentration of traps by reproducing the shape and position of the peaks in the TDS spectra and normalized the spectra shown in figure 2. The absolute amount of created traps in the first seven micrometers of the sample is determined by reproducing the NRA depth profiles after the D re-exposure at 600 K.

From the NRA depth profiles a constant D concentration level in the whole damaged zone is observed. The highest D concentration is obtained for the sample simultaneously damaged and

exposed to D at 450 K decreasing for higher temperatures but stabilizing for temperatures > 800 K. The TDS spectra show a single broad peak with a maximum at around 800 K, decreasing for simultaneous W/D exposures at higher temperatures. There is a distinct shoulder on the right side of the peak for the 450 K, 600 K and 800 K cases (above 1000 K) which disappears for the 900 K and 1000 K experiment (the desorption flux drops to zero before 1000 K). In general a similar single TDS peak was obtained in the case of sequential damaging at room temperature and exposed to D atoms at 600 K [20]. As can be seen in figure 2, the maximal concentration of deuterium in the damaged zone is reproduced within the experimental error bars by the simulation as well as the thickness of the damaged zone. Concerning the reproduction of the TDS spectra, we quantify the difference between simulations and experiments with the relative deviation between the experimental desorption rate (R_{exp}) and the simulated one (R_{sim}) defined as: $\epsilon = \frac{\int |R_{exp} - R_{sim}|}{\int R_{exp}}$. For this set of simulations, with only two traps in the damaged zone, the deviation is ϵ 7-12 % when considering only the main part of the TDS spectra (between 600 K and 1100 K). Considering the signal also above 1100 K would add another 2-3 % contribution to the relative deviation.
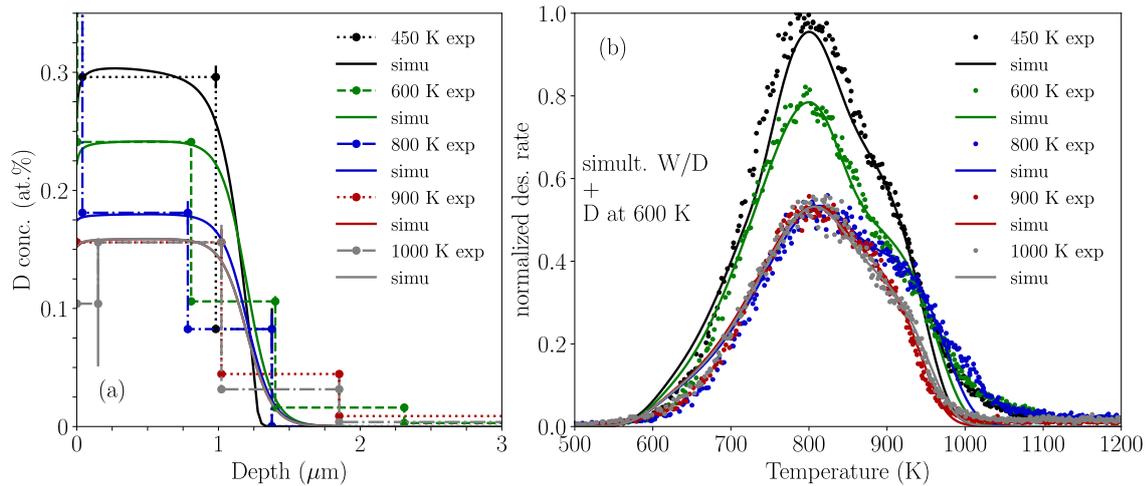

Figure 2. Comparison between the simulated and experimental NRA depth profiles (a) and TDS spectra (b) obtained for the simultaneous W/D exposure after decorating the defects with D at 600 K. The temperatures in the legends are the temperatures during the simultaneous W/D exposure.

b. Simultaneous W/D exposure

The determination of trapping parameters of the model i.e. de-trapping energies $E_{t,i}$ and trap concentrations n_i was shown in the previous sub-section, where the part of the simulation dedicated to the re-exposure to D atoms at 600 K and the following TDS is presented. The trapping parameters as determined for the self-damaged traps are given in table 1. In this sub-section, we present the simulated depth profiles obtained after the simultaneous W/D exposure and the cooling down step (before the D re-exposure at 600 K). Comparison between the simulated and measured deuterium depth profiles is shown in figure 3. The D concentration obtained from experiment decreases and the

D penetration depth increases with the W/D exposure temperature, being 0.1 µm for 450 K, 0.7 µm at 600 K and the whole damaging zone of 1 µm for higher temperatures.

The energy barriers at the surface control the concentration of mobile deuterium. Thus, they also control the total concentration of trapped deuterium and the depth reached by deuterium [17]. The energy barrier has already been determined in our previous work [17] for temperatures of 500 K and 600 K which guarantees the good agreement between the experimental and the simulated depth profiles for exposures at 450 K and 600 K. Especially, the depth profile at 450 K, in which the deuterium atoms do not migrate deeper than 0.1 µm, is well reproduced by the simulation. For the 600 K case, the agreement between simulation and experiment is good with respect to D concentration and migration depth. In both cases, and particularly for the 450 K exposure, the damaged layer is not fully filled with deuterium after 4 h of D exposure. Low temperature decreases not only the diffusivity but as will be shown later also the concentration of mobile particles in these experiments with low energy atoms which in turn also decreases the migration speed of deuterium into the bulk [12, 17].

In the case of the highest three temperatures of 800 K, 900 K and 1000 K the simulation shows that D atoms migrate throughout the whole damaging area in agreement with the experiment. The D bulk concentration as obtained by simulation is overestimated in the case of 800 K and underestimated in the case of 1000 K, but is in good agreement for the 900 K case. The disagreement for the two cases is due to the chosen monotonous evolution of $E_A(\theta)$ in the surface model [39] where it increases with θ. In order to have the same D concentration at 1 µm in the simulations and in the experiment it would require higher $E_A(\theta)$ at 800 K and lower $E_A(\theta)$ at 1000 K. However, such peaking affects the simulated TDS spectra which in turn would then not reproduce correctly the experimental ones. In addition, from our understanding, there is no obvious physical justification for such peaking.

Finally, for the highest three sample temperatures (800 K, 900 K and 1000 K), the simulations reproduce well the increase of the concentration of deuterium in the first 0.1 µm which is observed experimentally. In the simulations, this increase of the concentration is explained by the 3-minutes delay between the beginning of the cooling phase and the end of the D exposure. During these 3 minutes the exposure is still running while the temperature decreases. It leads to an extra D uptake up to 100 nm below the surface as the de-trapping/trapping balance changes with the temperature in favor of trapping.
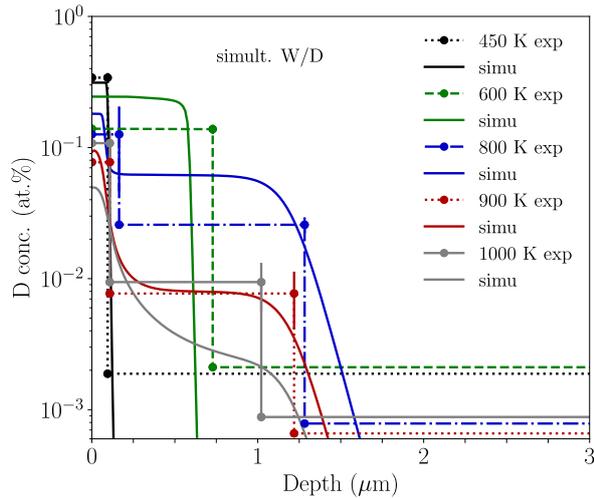
Figure 3. Comparison between the simulated and experimental D depth profiles after the simultaneous W/D exposure at the given temperatures during the experiments.

4.2 Simulation of sequential W-ion damaging at elevated temperatures and D-atom exposure

In this section, the free trapping parameters of the model are determined for the sequential W/D exposures. Again, in addition to two intrinsic traps, two self-damaged traps are added to the simulations. Since the D-atom exposure temperature in these experiments is 600 K, the intrinsic traps do not retain sufficient deuterium amount to give an apparent peak in the TDS spectra. As for the simulations of the simultaneous experiment, the shape of the TDS spectra and the position of the peaks give indication on the values of de-trapping energies and relative trap densities while the experimental D depth profiles give the absolute values for the total concentration of traps in the first seven micrometers. Figure 4 shows the comparison between experimental and simulated depth profiles (a) and TDS spectra (b). Similar to the simultaneous experiment the D depth profile is flat in the damaged zone, down to about 1 µm, and the D concentration decreases with the increase of the W-ion irradiation temperature systematically. Again, the simulated depth profiles reproduce the flat absolute concentration in the damaged zone as well as the thickness of the damaged layer. The TDS spectra are similar compared to the simultaneous W/D exposures, showing a single peak with a maximum at around 800 K. The peak is a bit narrower for the experiment at 1000 K as compared to other irradiation temperatures. For this set of simulations, if one considers only the main part of the TDS spectra between 600 K and 1100 K, the relative deviation is between 7 % and 15 %. In these deviation, the experimental tail at 1000 K accounts for 5 % (exposure at 300K, 600K and 1000 K) and 9% (exposure at 800 K where there is a small peak at 1050 K).
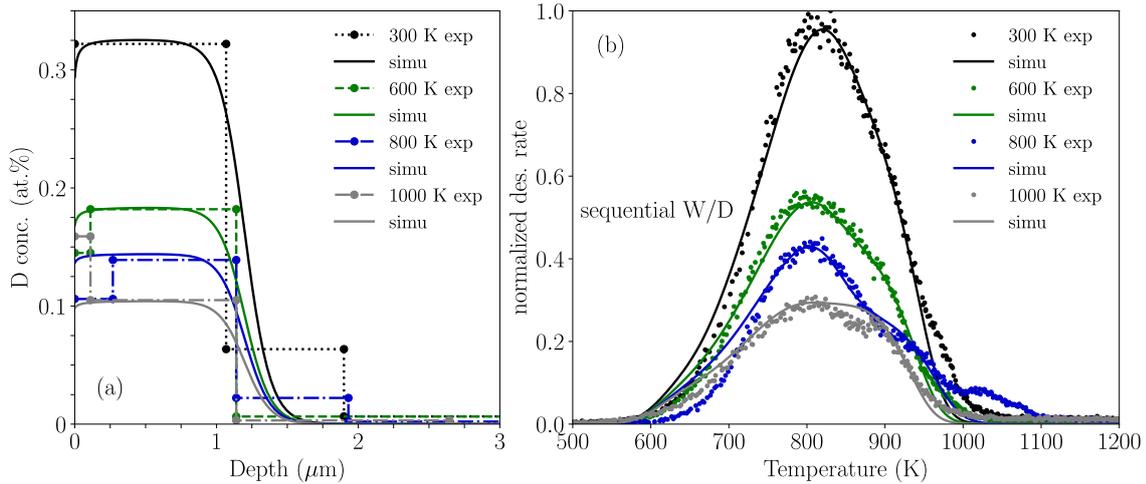
Figure 4. Comparison between the simulated and experimental NRA depth profiles (a) and TDS spectra (b) obtained after the sequential W/D exposure. The temperatures in the legends are the temperatures during W irradiation.

	Trap density	
Irradiation Temperature	Self-damaged trap 1 at.%	Self-damaged trap 2 at.%
Simultaneous W/D exposure		
450 K	0.205	0.110
600 K	0.160	0.085
800 K	0.100	0.080
900 K	0.095	0.065
1000 K	0.100	0.060
Sequential W/D exposure		
300 K	0.210	0.120
600 K	0.110	0.075
800 K	0.095	0.050
1000 K	0.045	0.060
De-trapping energy	$E_t = 1.83 \pm 0.05$ eV	$E_t = 2.10 \pm 0.06$ eV

Table 1. Temperatures during W irradiation, trap densities and de-trapping energies for the two self-damaged traps used in the simulations of simultaneous and sequential W/D exposure. The de-trapping energies E_t from the different simulations are averaged and their scattering around the average value is denoted by the accuracy in this table.

5. Discussion

In both sets of simulations - simultaneous and sequential W/D - two self-damaged traps have been used. The energies of these traps are in the range of those already published for various W damaging studies (with W ions [17, 20, 40, 41] and fission neutrons [42]).

The purpose of the simultaneous exposure study is to investigate the effects of the stabilization of self-damaged traps by deuterium during their creation. This has already been expressed by looking at the experimentally observed maximum concentrations of retained deuterium as function of the temperature of irradiation which were higher for the simultaneous W/D exposures compared to the sequential W/D exposures (see fig. 6 in [12]).

From the simulations, one can gain information on the total concentration of traps used to simulate the experimental results as well as the maximum concentration of mobile particles c_m during the simultaneous exposures. This quantity is particularly important since it might be the quantity driving the trap stabilizations. These two quantities are plotted in figure 5 together with the experimental maximum D concentrations for simultaneous W/D from 450 K to 1130 K. No experimental point exists for sequential W/D at 450 K. In addition, in the simultaneous W/D exposure at 450 K, the D atoms migrate only 0.1 µm deep which represent only 10 % of the damaged layer. Thus, we cannot say that there is any evidence that D atoms affect the traps deeper in the bulk at 450 K. For exposures above 600 K, the simultaneous W/D exposure leads to higher maximum D concentration (factor 1.3 at 600 K and 1.7 at 1000 K) compared to the sequential exposures (fig 5a). During simultaneous W/D exposures at 600 K, D migrates 0.7 µm deep (figure 3) which represents large part of the damaged layer. For simultaneous W/D exposures above 800 K, D migrates through all the damaged layer (figure 3). Thus, one can conclude that above 600 K, the presence of D affects the creation of traps. This effect seems to be especially pronounced at high temperature: the concentration of self-damaged traps is the same at 900 K and 1000 K.
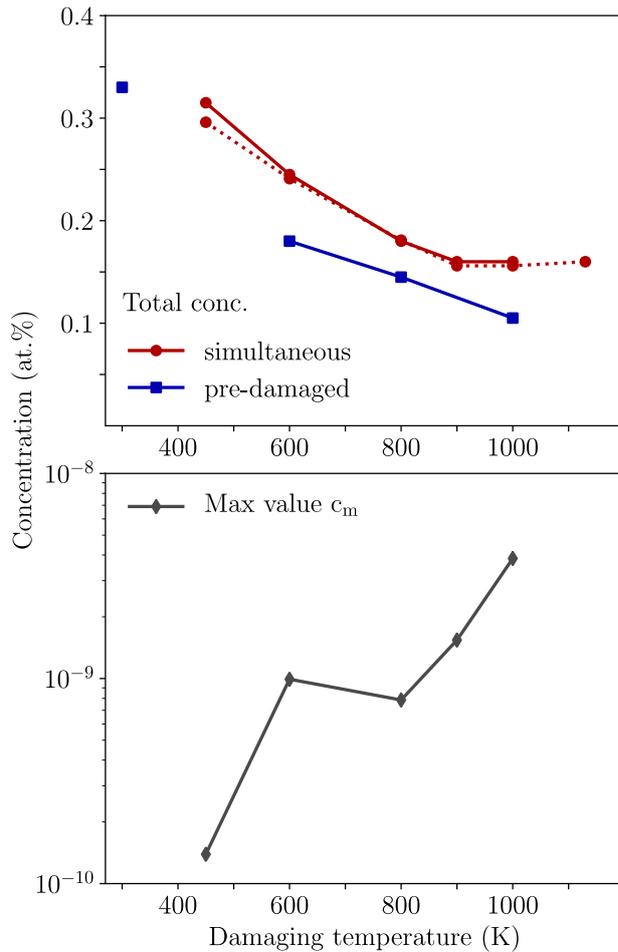
Figure 5. (a) Evolution of the total self-damaged trap concentrations (given by the simulations) with the sample temperature for simultaneous and sequential W/D. The dashed line gives the maximum values of the experimental D concentrations from 450 K to 1130 K for simultaneous W/D. (b) Evolution of the maximum concentration of mobile particles c_m with the exposure/irradiation temperature for the simultaneous exposure.

Except for an outlier at 600 K, c_m monotonically increases with increasing temperature (figure 5b).-If one compares to D ion implantations, there c_m is directly proportional to the incident flux of ions and inversely proportional to the diffusion coefficient [43, 44]: for a constant ion flux, c_m will decrease as a function of the temperature as the diffusion coefficient increases. The present behavior of D atom exposure looks similar to the Sievert's law behavior that would drive the concentration of the interstitial hydrogen for gas/H_2 exposure. Indeed, the Sievert's constant is given by the enthalpy difference (E_s) between hydrogen in H_2 and hydrogen in the metal which can also be calculated from the energy barrier as $E_s = E_A - E_D - E_R$ (when the dissociation energy is 0 eV) [45, 46]. Thus, the kinetically limiting process to reach the thermodynamic equilibrium are the ones occurring at the surface. The increase of interstitial D particles at higher temperatures can explain the large effect of the trap stabilization at high temperature (1000 K) which affects the evolution of the total concentration of self-damaged traps observed in figure 5.

With the help of the simulations, we can also go further and address the effect of deuterium on trap stabilization, trap by trap. To do that, the evolution of the trap concentration obtained from the simulation is plotted as function of the temperature of the experiment in figure 6 for the self-damaged trap 1 (a) and trap 2 (b).
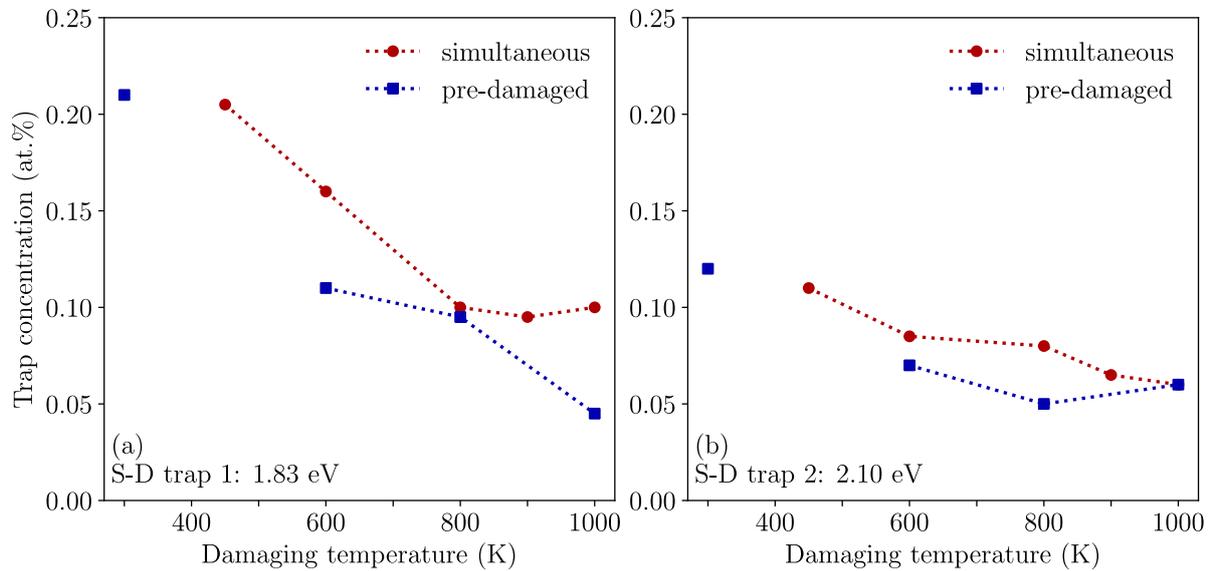

Figure 6. Comparison of trap concentrations used in the simulation of simultaneous and sequential W/D exposure for the self-damaged trap 1 (a) and trap 2 (b).

For all temperatures, the self-damaged trap 1 (E_t = 1.83 eV)has higher concentrations while exposing simultaneously D atoms and W ions, except 800 K temperature of irradiation(figure 6a). It shows that the presence of D atoms during the damaging reduces annihilation of the traps with increasing temperature. The trap stabilization is especially clear for the two highest temperatures. Indeed, between 800 K and 1000 K, if no D atoms are present to stabilize the traps, they are progressively annealed as the temperature rises up. This shows that the insertion of D atoms during the W irradiation reduces the annealing of this trap. In earlier simulation work [17], by comparing self-damaged trap 1 de-trapping energies to DFT calculations with various defects [21, 22, 35, 36, 37, 23, 24, 47, 48, 49], self-damaged trap 1 has been attributed to dislocation loop. On another hand, Gorodetsky [50] suggests that one can determine the de-trapping energy of H from big vacancy clusters by considering H on a free surface. Following DFT data [22, 35, 36, 37], it ranges from 1.65 eV to 2.36 eV. Gorodetsky also suggests that the binding energy of hydrogen with a vacancy cluster increases as the vacancy cluster increases: self-damaged trap 1 could also be attributed to small vacancy clusters. The stabilization of both types of defects could be done via the 'jog-punching' mechanism described in [49, 51, 52] which can eventually lead to bubbles formation [52] or loop punching [53]. Another possible explanation for the stabilization of the small vacancy clusters is given in the next paragraph based on the increase of the migration barrier of vacancies containing H [21, 54].

The stabilization of self-damaged trap 2 (E_t = 2.10 eV) is less obvious than for the self-damaged trap 1 except maybe for exposure at 800 K (figure 6b). Following the Gorodetsky model

[50], one can attribute self-damaged trap 2 to vacancy clusters [17]. In the sequential case, the concentration of this trap increases between 800 K and 1000 K. Such increase has already been reported in previous simulations [17] when the exposed damaged samples were pre-annealed at various temperatures. It has been related to growth of the vacancy clusters during the annealing process. Such growth is not observed in simultaneous exposure which can be explained by the increased migration barrier of vacancies containing H [21, 54]. The presence of high concentration of solute D that can feed mono-vacancies and small vacancy clusters at 900 K and 1000 K might spoil the growth of large vacancy clusters. The higher concentration of self-damaged trap 2 at 800 K is then the result of a balance between an increased source of vacancy (from the stabilization by D) and growth of vacancy clusters. One can also suggest again the 'jog-punching' mechanism [49, 51, 52] that can lead to the growth of bubbles along dislocations.

The stabilization of traps induced by the presence of hydrogen evidenced here might have an important effect on the total amount of tritium that a W divertor target can accommodate during ITER operation. Recent simulations predict that the tritium retention in the W divertor target is higher in neutron-damaged material than in material not damaged by neutrons [5]. The ratio damaged/undamaged can reach 30 in the hotter area where the temperature can reach 1000 K or more. Thus, the stabilization of the traps presented in this paper, that was not taken into account in the tokamak cycle simulations presented in [5], will enhance the retention in damaged W especially at the strike point position where the temperature is the highest (and so, where the stabilization is the most efficient according to the present data). Here we got a factor of 1.3-1.5 increase in D atom concentration when comparing the D retention for simultaneous and sequential experiment over the whole studied temperature range. This means that even at the ITER or DEMO relevant temperatures of around 1000 K – 1300 K near the strike points there will be this difference in HI retention due to the presence of hydrogen. However, the HI fluxes of ions and neutrals to the walls of a reactor will be few orders of magnitude higher (10^{21}-10^{24} particles/cm^{2}s) as compared to the present study (5.4×10^{18} D/m^{2}s). This will increase the concentration of mobile HI atoms in the bulk of the material. How the increase in concentration of the mobile particles influences the stabilization of traps needs further studies. To have a complete picture of the effect of neutron irradiation on tritium retention during nuclear operation of ITER and DEMO, one also needs to take into account nuclear transmutation that will lead to formation of various impurities in the bulk (He, Re, Os …) [55]. Each of these transmutation products could also impact fuel retention as HI can bind to them [23, 56] (even though their binding energy with hydrogen is weak). In addition, they can also impact the formation and motion of defect such as dislocations [56, 57].

17

6. Conclusion

The effect of the presence of hydrogen isotope on defect evolution was studied by modeling by the MHIMS code two experiments: sequential and simultaneous W/D exposure. By modeling D depth profiles and D desorption spectra we could determine the de-trapping energies and trap concentrations for different temperatures of the experiments. In order to model the simultaneous experiment a model of trap creation during the D-atom exposure was implemented into the MHIMS code. The experimental strategy was chosen such that trap concentrations for simultaneous and sequential exposures could be directly compared. Two different traps were necessary to model D depth profiles and D desorption spectra. The de-trapping energies were found to be the same for sequential and simultaneous W/D exposure. The comparison of trap concentrations for simultaneous and sequential W/D exposure gives us direct evidence on the effect of presence of mobile D on trap evolution. This was directly evaluated in this paper. The first trap with 1.83 eV de-trapping energy being attributed to dislocation loops or small vacancy cluster is higher for simultaneous experiment at all temperatures whereas the 2.10 eV trap is less affected by the experimental procedure and presence of HI. We believe that this effect is not specific on the hydrogen isotope used and can be used for extrapolation to tritium.

Acknowledgement

References

[1]   V. Chan, R. Stambaugh, A. Garofalo, J. Canik, J. Kinsey and et al., "A fusion development facility on the critical path to fusion energy," *Nucl. Fusion,* vol. 51, no. 8, p. 083019, 2011.

[2]   J. Roth, E. Tsitrone, A. Loarte, T. Loarer, R. Neu, V. Philipps and S. Brezinsek, "Recent analysis of key plasma wall interactions issues for ITER," *J. Nucl. Mater.,* vol. 390–391, no. 1., p. 1–9, 2009.

[3]   . G. Federici, J. Brooks, D. Coster and G. Janeschitz et al., "Assessment of erosion and tritium codeposition in ITER-FEAT," *J. Nucl. Mater.,* Vols. 290-293, pp. 260-265, 2001.

[4] J.-H.You, "A review on two previous divertor target concepts for DEMO: mutual impact between structural design requirements and materials performance," *Nucl. Fusion,* vol. 55, no. . , (2015)., p. 113026, 2015.

[5] E. A. Hodille, E. Bernard, S. Markelj, J. Mougenot, C. S. Becquart, R. Bisson and C. Grisolia, "Estimation of the tritium retention in ITER tungsten divertor target using macroscopic rate equations simulations," *Phys. Scr. ,* vol. T170, p. 014033, 2017.

[6] B. Wirth, K. Nordlung, D. Whyte and D. Xu, "Fusion materials modeling: Challenges and opportunities," *MRS Bulletin,* vol. 36, p. 216–222, 2011.

[7] J. Marian and e. al, "Recent advances in modeling and simulation of the exposure and response of tungsten to fusion energy conditions," *Nucl. Fusion,* vol. 57, p. 092008, 2017.

[8] W. R. Wampler and R. P. Doerner, "The influence of displacement damage on deuterium retention in tungsten exposed to plasma," *Nucl. Fusion,* vol. 49, p. 115023, 2009.

[9] Y. Hatano, M. Shimada, T. Otsuka, Y. Oya and V. K. Alimov, "Deuterium trapping at defects created with neutron and ion irradiations in tungsten," *Nucl. Fusion,* vol. 53, p. 073006, 2013.

[10] O. V. Ogorodnikova, Y. Gasparyan, V. Efimov, Ł. Ciupiński and J. Grzonka, "Annealing of radiation-induced damage in tungsten under and after irradiation with 20 MeV self-ions," *J. Nucl. Mater.,* vol. 451, no. 1-3, pp. 379-386, 2014.

[11] O. V. Ogorodnikova and V. Gann, "Simulation of neutron-induced damage in tungsten by irradiation with energetic self-ions," *J. Nucl. Mater.,* vol. 460, p. 60, 2015.

[12] S. Markelj, T. Schwarz_Selinger, A. Zaloznik, M. Kelemen, P. Vavpetic, P. Pelicon, E. Hodille and C. Grisolia, "Deuterium retention in tungsten simultaneously damaged by high energy W ions and loaded by D atoms," *Nucl. Mater. Energ.,* vol. 12, pp. 169-174, 2017.

[13] E. A. Hodille, X. Bonnin, R. Bisson, T. Angot, C. S. Becquart, J.-M. Layet and C. Grisolia, "Macroscopic rate equation modeling of trapping/detrapping of hydrogen isotopes in tungsten materials," *J. Nucl. Mater. ,* vol. 467, pp. 424-431, 2015.

[14] S. Markelj, A. Založnik, T. Schwarz-Selinger, O. V. Ogorodnikova, P. Vavpetič, P. Pelicon and I. Čadež, "In situ NRA study of hydrogen isotope exchange in self-ion damaged tungsten exposed to neutral atoms," *J. Nucl. Mater.,* vol. 469, p. 133–144, 2016.

[15] E. Salancon, T. Dübeck, T. Schwarz-Selinger, F. Genoese and W. Jacob, "Redeposition of amorphous hydrogenated carbon films during thermal decomposition," *J. Nucl. Mater. 376,* pp. 160-168, 2008.

[16] P. Wang, W. Jacob, L. Gao, T. Dürbeck and T. Schwarz-Selinger, "Comparing deuterium retention in tungsten films measured by temperature programmed desorption and nuclear reaction analysis," *Nucl. Inst. Meth. Phys. Res. B ,* vol. 300, p. 54–61, 2013.

[17] E. A. Hodille, A. Založnik, S. Markelj, T. Schwarz-Selinger, C. S. Becquart, R. Bisson and C. Grisolia, "Simulations of atomic deuterium exposure in self-damaged tungsten," *Nucl. Fusion,* vol. 57, p. 056002, 2017.

[18] G. R. Longhurst, "TMAP-7 user manual," Idaho National Laboratory Report, INEEL.EXT-04-2004, 2004.

[19] K. Schmid, V. Rieger and A. Manhard, "Comparison of hydrogen retention in W and W/Ta alloys," *J. Nucl. Mater. ,* vol. 426, pp. 247-253, 2012.

[20] A. Zaloznik, S. Markelj, T. Schwarz-Selinger and K. Schmid, "Deuterium atom loading of self-damaged tungsten at different sample temperatures," *J. Nucl. Mater.,* vol. 496, pp. 1-8, 2017.

[21] N. Fernandez, Y. Ferro and D. Kato, "Hydrogen diffusion and vacancies formation in tungsten: Density Functional Theory calculations and statistical models," *Acta Mater. ,* vol. 94, pp. 307-318, 2015.

[22] D. F. Johnson and E. A. Carter, "Hydrogen in tungsten: Absorption, diffusion, vacancy trapping,

and decohesion," *J. Mater. Res.,* vol. 25, no. 2, p. 315, 2010.

[23] K. Heinola, T. Ahlgren, K. Nordlund and J. Keinonen, "Hydrogen interaction with point defects in tungsten," *Phys. Rev. B ,* vol. 82, p. 094102, 2010.

[24] Y.-L. Liu, H.-B. Zhou and Y. Zhang, "Investigating behaviors of H in a W single crystal by first-principles: From solubility to interaction with vacancy," *J. Alloys Compd. ,* vol. 509, pp. 8277-8282, 2011.

[25] K. Schmid, J. Bauer, T. Schwarz-Selinger, S. Markelj, U. v Toussaint, A. Manhard and W. Jacob, "Recent progress in the understanding of H transport and trapping in W," *Phys. Scr. ,* vol. T170, p. 014037, 2017.

[26] O. V. Ogorodnikova, J. Roth and M. Mayer, "Deuterium retention in tungsten in dependence of the surface conditions," *J. Nucl. Mater. ,* Vols. 313-316, pp. 469-477, 2003.

[27] A. Založnik, S. Markelj, T. Schwarz-Selinger, Ł. Ciupiński, J. Grzonka, V. P. and P. Pelicon, "The influence of the annealing temperature on deuterium retention in self-damaged tungsten," *Phys. Scr.,* vol. T167, p. 014031, 2016.

[28] M. H. J. 't Hoen, B. Tyburska-Püschel, K. Ertl, M. Mayer, J. Rapp, A. W. Kleyn and P. A. Zeijmans van Emmichoven, "Saturation of deuterium retention in self-damaged tungsten exposed to high-flux plasmas," *Nucl. Fus.,* vol. 52, p. 023008, 2012.

[29] V. Alimov, Y. Hatano, B. Tyburska-Püschel, K. Sugiyama, I. Takagi, Y. Furuta, J. Dorner, M. Fußeder, K. Isobe, T. Yamanishi and M. Matsuyama, "Deuterium retention in tungsten damaged with W ions to various damage levels," *J. Nucl. Mater.,* vol. 441, p. 280–285, 2013.

[30] T.-U. Nahm and R. Gomer, "The adsorption of hydrogen on W(110) and Fe covered by W(110)," *Surf. Sci. ,* vol. 375, pp. 281-292, 1997.

[31] P. W. Tamm and L. D. Schmidt, "Binding States of hydrogen on tungsten," *J. Chem. Phys. ,* vol. 54, p. 4775, 1971.

[32] S. Markelj, O. V. Ogorodnikova, P. Pelicon, T. Schwarz-Selinger and I. Cadez, "Temperature dependence of D atom adsorption on polycrystalline tungsten," *Appl. Surf. Sci. ,* vol. 282, pp. 478-486, 2013.

[33] A. Nojima and K. Yamashita, "A theoretical study of hydrogen adsorption and diffusion on a W(110) surface," *Surf. Sci. ,* vol. 601, pp. 3003-3011, 2007.

[34] Z. A. Piazza, M. Ajmalghan, Y. Ferro and R. D. Kolasinski, "Saturation of tungsten surfaces with hydrogen: A density functional theory study complemented by low energy ion scattering and direct recoil spectroscopy data," *Acta Mater.,* vol. 145, pp. 388-398, 2018.

[35] K. Heinola and T. Ahlgren, "First-principles study of H on the reconstructed W(100) surface," *Phys. Rev. B ,* vol. 81, p. 073409, 2010.

[36] A. Moitra and K. Solanki, "Adsorption and penetration of hydrogen in W: A first principles study," *Comp. Mater. Sci. ,* vol. 50, pp. 2291-2294, 2011.

[37] P. Ferrin, S. Kandoi, A. Udaykumar Nilekar and M. Mavrikakis, "Hydrogen adsorption and diffusion on and in transition metal surfaces: A DFT study," *Surf. Sci. ,* vol. 606, pp. 679-689, 2012.

[38] Fraunfelder, "Solution and Diffusion of Hydrogen in Tungsten," *J. Vac. Sci. Tech.,* vol. 6, p. 388, 1968.

[39] E. A. Hodille, S. Markelj, T. Schwarz-Selinger, A. Zaloznik, M. Pecovnik, M. Kelemen and C. Grisolia, "Coverage dependent surface energies in kinetic surface models for the desorption and absorption of hydrogen on tungsten," *To be submitted,* 2018.

[40] O. V. Ogorodnikova, "Fundamental aspects of deuterium retention in tungsten at high flux plasma exposure," *J. Appl. Phys. ,* vol. 118, p. 074902, 2015.

[41] M. 't Hoen, M. Mayer, A. Kleyn, H. Schut and P. Zeijlmans van Emmichoven, "Reduced deuterium

retention in self-damaged tungsten exposed to high-flux plasmas at high surface temperatures," *Nucl. Fusion,* vol. 53, p. 043003, 2013.

[42] M. Shimada, G. Gao, Y. Hatano, T. Oya, M. Hara and P. Calderoni, "The deuterium depth profile in neutron-irradiated tungsten exposed to plasma," *Phys. Scr. ,* vol. T 145, p. 014051, 2011.

[43] L. Gao, W. Jacob, U. von Toussaint, A. Manhard, M. Balden, K. Schmid and T. Schwarz-Selinger, "Deuterium supersaturation in low-energy plasma-loaded tungsten surfaces," *Nucl. Fusion 57,* p. 016026, 2017.

[44] E. A. Hodille, N. Fernandez, Z. A. Piazza, M. Ajmalghan and Y. Ferro, "Hydrogen supersaturated layers in H/D plasma-loaded tungsten: A global model based on thermodynamics, kinetics and density function theory data," *Phys. Rev. Mater. 2,* p. 093802, 2018.

[45] M. A. Pick and K. Sonnenberg, "A model for atomic hydrogen-metal interactions-application to recycling, recombination and permeation," *J. Nucl. Mater.,* vol. 131, pp. 208-220, 1985.

[46] J. W. Davenport, G. J. Dienes and R. A. Johnson, "Surface effects on the kinetics of hydrogen absorption by metals," *Phys. Rev. B,* vol. 25, no. 4, pp. 2165-2174, 1982.

[47] W. Xiao and W. T. Geng, "Role of grain boundary and dislocation loop in H blistering in W: A density functional theory assessment," *J. Nucl. Mater. ,* vol. 430, pp. 132-136, 2012.

[48] A. Bakaev, P. Grigorev, D. Terentyev, A. Bakaeva, E. E. Zhurkin and A. Mastrikov, "Trapping of hydrogen and helium at dislocations in tungsten: an ab-initio study," *Nucl. Fusion 57,* p. 126040, 2017.

[49] D. Terentyev, V. Dubinko, A. Bakaev, Y. Zayachuk, W. Van Renterghem and P. Grigorev, "Dislocations mediate hydrogen retention in tungsten," *Nucl. Fusion ,* vol. 54, p. 042004, 2014.

[50] A. E. Gorodetsky, A. P. Zakharov, V. M. Sharapov and V. K. Alimov, "Interaction of hydrogen with radiation defects in metals," *J. Nucl. Mater. ,* Vols. 93-94, pp. 588-593, 1980.

[51] P. Grigorev, D. Terentyev, G. Bonny, E. E. Zhurkin, G. Van Oost and J.-M. Neterdaeme, "Interaction of hydrogen with dislocations in tungsten: An atomistic study," *J. Nucl. Mater. ,* vol. 465, pp. 364-372, 2015.

[52] P. Grigorev, D. Terentyev, V. Dubinko, G. Bonny, G. Van Oost, J.-M. Noterdaeme and E. E. Zhurkin, "Nucleation and growth of hydrogen bubbles on dislocations in tungsten under high flux low energy plasma exposure," *Nucl. Inst. Meth. Phys. Res. B ,* vol. 352, pp. 96-99, 2015.

[53] V. I. Dubinko, P. Grigorev, A. Bakaev, D. Terentyev, G. Van Oost, F. Gao, D. Van Neck and E. E. Zhurkin, "Dislocation mechanism of deuterium retention in tungsten under plasma implantation," *J. Phys.: Condens. Matter ,* vol. 26, p. 395001, 2014.

[54] P. Hautojärvi, H. Huomo, M. Puska and A. Vehanen, "Vacancy recovery and vacancy-hydrogen interaction in niobium and tantalum studied by positrons," *Phys. Rev. B,* vol. 32, no. 7, pp. 4326-4331, 1985.

[55] M. R. Gilbert and J.-C. Sublet, "Neutron-induced transmutation effects in W and W-alloys in a fusion environment," *Nucl. Fusion 51,* p. 043005, 2011.

[56] G.-H. Lu, H.-B. Zhou and C. S. Becquart, "A review of modelling and simulation of hydrogen behaviour in tungsten at different scales," *Nucl. Fusion,* vol. 54, p. 086001, 2014.

[57] H. Li, S. Wurster, C. Motz, L. Romaner, C. Ambrosch-Draxl and R. Pippan, "Dislocation-core symmetry and slip planes in tungsten alloys: Ab-initio calculations and microcantilever bending experiments," *Acta Mater.,* vol. 60, no. 2, pp. 748-758, 2012.